11

Thermodynamics of Self-Assembly

L. Magnus Bergström
Royal Institute of Technology
Sweden

1. Introduction

Self-assembly of molecules to form much larger colloidal or nanosized aggregates has received a great deal of attention the last decades or so and the number of technical applications and products based on the principle of self-assembly is still rapidly increasing. Moreover, fundamental processes in life sciences such as the properties and stability of lipid membranes and their interactions with proteins, DNA etc are based on the phenomenon of self-assembly.

In this chapter we outline the fundamental principles of the thermodynamics of self-assembling molecules into self-associated colloidal aggregates and interfaces. Since the process of self-assembling molecules implies an increase of order in a system, this process must be unfavourable from an entropic point of view. Consequently, in the absence of any additional interactions or driving forces, molecules that interact favourable with solvent molecules do mix completely as one single phase of free molecules dispersed in a solvent. On the other hand, the presence of a driving force that is strong enough to overcome the unfavourable entropy may lead to a spontaneous self-assembly of molecules. In the present work, we mainly focus on the technically and biologically important case of self-assemblies formed by amphiphilic molecules, i.e. molecules composed of one hydrophilic and one hydrophobic part. The driving force for the self-association of amphiphilic molecules in an aqueous solvent is the hydrophobic effect, i.e. the principle preventing oil and water to mix in a liquid phase. As a result, under certain conditions amphiphilic molecules may spontaneously form a single disperse phase of thermodynamically stable self-associated interfaces, in addition to the options available for ordinary (non-amphiphilic) molecules, i.e. either to completely mix as free solute molecules with the solvent or to separate into two or more liquid phases.

Below it is demonstrated that, by means of combining thermodynamics of self-assembly with the bending elasticity approach of calculating the free energy of a single self-associated interface, it is possible to rationalize the geometrical size and shape of self-assembled interfaces in terms of the chemical architecture of the constituting amphiphilic molecules (size of hydrophilic and hydrophobic part, respectively, charge number, flexibility etc) as well as solution properties (salinity, temperature etc).

2. Amphiphilic molecules

Amphiphilic molecules consist of a hydrophilic head group and a hydrophobic tail and may roughly be subdived into different types: (*i*) Surfactants usually have a moderately sized tail

and do form rather small globular or long wormlike or threadlike self-assembled interfaces, called micelles, in an aqueous solvent. (*ii*) Lipids have a much larger hydrophobic part as compared to the head group and form comparatively large bilayer structures. As a common notation in the present work, we refer to micelles and bilayers as self-assembled interfaces. The head groups may be either charged (ionic surfactants) or uncharged (nonionic surfactants). Many lipids are zwitter-ionic, i.e. they have a head group that consists of both positive and negative charges whereas the whole molecule lacks a net charge. The driving force needed for amphiphilic molecules to spontaneously self-assemble into micelles and bilayers is usually denoted the hydrophobic effect, i.e. the principle that hydrocarbon (oil) and water do not mix. As a result, in order to reduce the hydrocarbon-water contact in an aqueous solution the hydrophobic tails self-assemble to form liquid-like cores with the head groups located at the aggregate interface pointing towards the aqueous bulk solvent phase. Any quantitative molecular theory that accurately describes the hydrophobic effect is unfortunately not available, but it is generally believed that water molecules in the proximity of hydrophobic surfaces form entropically unfavourable ordered structures (clathrates). (Evans & Wennerström, 1994) Nevertheless, rather accurate semi-empirical expressions have been generated for the hydrophobic free energy of bringing hydrocarbon chains from an aqueous solution to the corresponding hydrocarbon liquid bulk phase using solubility data for hydrocarbons in water. (Tanford, 1980)

The hydropobic effect, together with some partly counteracting contributions to micelle formation, may be incorporated into a single free energy parameter $\Delta\mu_{mic}$ that may be interpreted as the free energy per aggregated molecule of forming a micelle out of free surfactant molecules [see Section 4 below]. The most important contributions to $\Delta\mu_{mic}$, in addition to the hydrophobic effect, are chain conformational entropy (Ben-Shaul et al., 1985; Gruen, 1985), electrostatics and excluded volume repulsive interactions among the surfactant head groups. The hydrophobic effect and chain conformational entropy are related to the surfactant tails whereas electrostatics and excluded volume repulsion are related to the surfactant head groups.

The electrostatic free energy contribution is essential for surfactant aggregates consisting of at least one ionic surfactant. It appears to be mainly a result of the unfavourable entropic effect of concentrating counter-ions in a diffuse layer outside charged aggregate interfaces. An accurate explicit expression of the electrostatic free energy have been derived, as an expansion to second order in curvature of the charged surface, from the Poisson-Boltzmann theory. (Mitchell & Ninham, 1989)

An additional repulsive free energy contribution arises as solvent molecules penetrate and mix with the hydrophilic head groups. The resulting excluded volume repulsion among the surfactant head groups increases in magnitude with head group volume. For nonionic surfactants this is the main free energy contribution related to the head groups, counteracting free energy contributions related to the tails and making the molecule amphiphilic in nature. (Bergström, 2009).

3. Entropy of self-assembly

The ideal entropy of mixing N free amphiphilic molecules with N_w solvent molecules is given by the expression

$$S_{free} = -k\left(N_w \ln\phi_w + N \ln\phi_{free}\right) \tag{1}$$

where ϕ_w and ϕ_{free} are the volume fractions of solvent and solute, respectively, and k is Boltzmann's constant. Eq. (1) is a general expression in the sense that it allows for the mixing of solute and solvent with different molecular volumes. (Guggenheim, 1952; Flory, 1974) For the special case of equal molecular volumes, volume fractions may be replaced with mole fractions in Eq. (1).

Now, consider the process of self-assembling N free amphiphilic molecules to form a single aggregate or self-assembled interface. Since the self-assembling process is associated with an ordering of molecules, there is a change in entropy as a result of this process. The entropy of mixing one single aggregate with solvent molecules is given by

$$S_{agg} = -k\left(N_w \ln \phi_w + \ln \phi_N\right) \tag{2}$$

Hence, the entropy change per aggregate formed in the process of self-assembly may be obtained by subtracting Eq. (1) from Eq. (2), i.e.

$$\Delta S_{agg} \equiv S_{agg} - S_{free} = -k\left(\ln \phi_N - N \ln \phi_{free}\right) \tag{3}$$

Usually $\ln\phi_N$ and $\ln\phi_{free}$ are about the same order of magnitude [see further below], and Eq. (3) may be approximately simplified so as to give

$$\Delta S_{agg} \approx kN \ln \phi_{free} \tag{4}$$

for the case $N >> 1$.

We note that $\Delta S_{agg} < 0$ and, as expected, the increase in order due to the process of self-association implies a reduction in overall entropy. This means that ordinary molecules that interacts more or less favourable with solvent molecules will not spontaneously self-assemble, but prefer to remain as free molecules in a close to ideal mixture. Moreover, it becomes clear from Eq. (4) that the entropic driving force of dissociating molecules increases with decreasing solute concentration ϕ_{free}. As will be further discussed below, this entropic contribution is utmost important as to determine the equilibrium size of self-assembled interfaces.

4. Multiple equilibrium

From a thermodynamic point of view, a spontaneous self-assembly process may be written as a set of reactions, one for each value of N, i.e.

$$N \text{ molecules} \rightarrow A_N \tag{5}$$

The total free energy of the processes can then be written as a sum of the "interaction" free energy of forming a micelle ($= N\Delta\mu_{mic}$) and the unfavourable free energy of self-assembling amphiphilic molecules ($\Delta G_{agg} = -T\Delta S_{agg} > 0$, where T is the absolute temperature), giving the following multiple set of equilibrium conditions

$$\Delta G_{tot} = N\Delta\mu_{mic} + \Delta G_{agg} = 0 \tag{6}$$

It follows from Eq. (6) that $\Delta\mu_{mic} < 0$ must be a necessary condition for the process to overcome the unfavourable entropy of self-association ($\Delta S_{agg} < 0$). As previously mentioned,

it is mainly the hydrophobic effect that accounts for negative values of $\Delta\mu_{mic}$, the remaining contributions discussed above having slightly counteracting positive contributions to $\Delta\mu_{mic}$. (Eriksson et al., 1985)
From Eq. (3) it now follows that

$$\Delta G_{agg} = kT\left(\ln\phi_N - N\ln\phi_{free}\right) \tag{7}$$

and by combining Eqs. (6) and (7) we may write the set of equilibrium conditions in the following way

$$\Delta G_{tot} = N\left(\Delta\mu_{mic} - kT\ln\phi_{free}\right) + kT\ln\phi_N = 0 \tag{8}$$

It will become clear throughout this chapter that Eq. (8) is the central thermodynamic relationship when the spontaneous and reversible process of self-assembling amphiphilic molecules is due to be rationalized.

5. Critical micelle concentration

In order to achieve a full equilibrium in accordance with Eq. (8), the surfactant molecules exchange more or less rapidly between the self-assemblies and as free molecules in the surrounding bulk solution. The latter may be considered as a large reservoir where environmental variables defining the solution state, e. g. temperature, pressure, chemical potentials of the free surfactant molecules etc, are kept constant during the reversible process of self-assembly. (Eriksson et al., 1985; Israelachvili, 1991) One important consequence of this thermodynamic equilibrium situation, and the multiple equilibrium approach inherent in Eq. (8), is that the entropic dissociation driving force in Eq. (4) is too large at low surfactant concentrations for self-assembled interfaces with comparatively large N to be present. As a result, self-assembled interfaces will only form above a certain concentration of surfactant, and above this concentration limit both free surfactants and self-assembled interfaces must coexist simultaneously in a dispersed surfactant solution.
The volume fraction of self-assembled interfaces (ϕ_N) and free surfactant (ϕ_{free}), respectively, are plotted against the overall surfactant volume fraction (= $\phi_{free} + \phi_N$) in Fig. 1. It is clearly seen that the aggregate concentration is virtually zero below a certain value of the total surfactant concentration, whereas above this value the aggregate concentration increases proportionally to the surfactant concentration ($\phi_{free} + \phi_N$), with ϕ_{free} approximately constant. This threshold value is called the critical micelle concentration (CMC).
The appearance of the curves in Fig. 1 may be rationalized as follows: at low surfactant concentration (i.e. below CMC), ϕ_{free} is small and $-kT\ln\phi_{free} \gg -\Delta\mu_{mic}$ (note that both quantities on either side of the inequality sign are positive quantities). As a result, the term including $\Delta\mu_{mic}$ in Eq. (8) becomes negligible and, as a consequence, $\phi_N = \phi_{free}^N \ll \phi_{free}$. As a result, the concentration of higher order aggregates (dimers, trimers etc.) rapidly becomes negligible as N increases beyond unity. As the surfactant concentration increases, the quantity of $-kT\ln\phi_{free}$ will eventually be of the same order of magnitude as $-\Delta\mu_{mic}$. However, we may neglect the term including ϕ_N, since $-NkT\ln\phi_{free} \gg -kT\ln\phi_N$ in so far $N >> 1$. As a result, Eq. (8) may be simplified so as to give

$$\Delta\mu_{mic} \approx kT \ln \phi_{free} \tag{9}$$

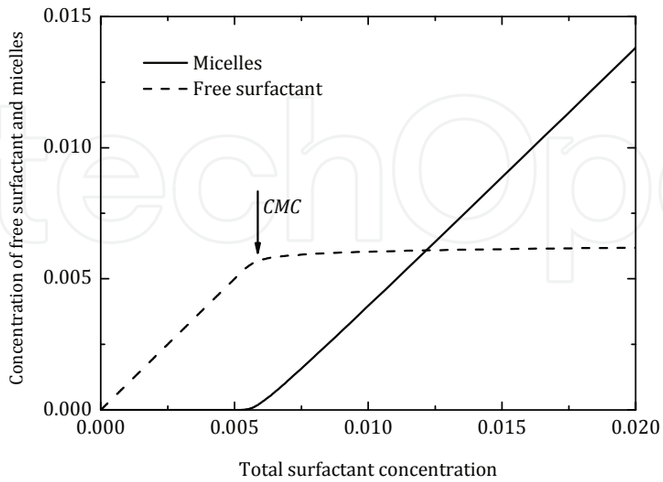

Fig. 1. The volume fraction of micelles (ϕ_N, solid line) and free surfactant (ϕ_{free}, dashed line) plotted against the overall surfactant volume fraction ($\phi_{free} + \phi_N$). The free energy was set equal to $\Delta\mu_{mic} = -5kT$ giving a $CMC \approx 0.0055$ (in volume fraction units)

Since ϕ_{free} is approximately constant above *CMC*, we obtain the following well-known and important relation between *CMC* (which is straightforward to measure) and the micelle "interaction" free energy

$$\Delta\mu_{mic} = kT \ln CMC \tag{10}$$

Eq. (10) is frequently claimed to follow from the so called "pseudo phase separation-model". However, from our present treatment it is perfectly clear that Eq. (10) follows straightforwardly from conventional solution thermodynamics as an approximation that becomes increasingly valid in the limit of large aggregation numbers ($N >> 1$). The smallest micelles observed to be formed by conventional surfactants have aggregation numbers about $N = 50$, which appears to be a sufficiently large number for Eq. (10) to be, for all practical purposes, accurate.

5.1 Dependence of CMC on molecular architecture and solution properties

CMC depends strongly on the molecular architecture of amphiphilic molecules. In particular, CMC decreases considerably with increasing size of the hydrophobic tail. For surfactants with tails consisting of aliphatic hydrocarbon alkyl chains C_nH_{2n+1}, the logarithm of CMC has been found to follow a linear relationship (sometimes referred to as the Shinoda equation), i.e.

$$\ln CMC = A - Bn \tag{11}$$

where A and B are two constants. For ionic surfactants, the slope has been experimentally found to equal $B \approx 0.7$, whereas $B \approx 1.1$ for nonionic surfactants and $B \approx 1.5$ for alkanes (corresponding to solubility rather than CMC, since alkanes are not amphiphilic). (Shinoda

et al., 1963; Israelachvili, 1991; Jönsson et al., 1998) The latter value corresponds to what is expected from the empirical contribution to $\Delta\mu_{mic}$ due to the hydrophobic effect for aliphatic hydrocarbon chains ($\Delta\mu_{mic}^{hb} = -2.0 - 1.5n$). (Tanford, 1980) The reduction of B for ionic and nonionic surfactants may be rationalized as a result of the contributions due to electrostatics and excluded head group volume repulsion to $\Delta\mu_{mic}$. In particular, the electrostatic free energy increases significantly as the electrolyte concentration of free surfactant is reduced with the lowering of CMC. As a consequence, the lowering of $\Delta\mu_{mic}$ with n becomes strongly counteracted and B significantly reduced. Upon adding additional salt to an ionic surfactant mixture, B increases so as to approach the value observed for nonionic surfactants.

The reduction of electrostatic free energy with increasing electrolyte concentration also causes a strong CMC dependence of ionic surfactants on the concentration of added salt. It appears that, at moderate and high salt concentrations (c_{salt}), CMC approximately follows the linear relation (Shinoda et al., 1963)

$$\ln CMC = constant - B' \ln c_{salt} \tag{12}$$

where the constant $B' = 0.5\text{-}1.0$, depending mainly on the size of the surfactant aggregates. The approximate mathematical form of Eq. (12), as well at the value of B', may be accurately reproduced by calculations of the electrostatic free energy from the Poisson-Boltzmann theory.

The CMC of nonionic surfactants display a slight dependence on head group volume (CMC increases with increasing size of the head group) as a result of excluded volume interactions. More significant, however, appears to be the temperature dependence of CMC of nonionic surfactants consisting of an ethylene oxide based head group. The ethylene oxide group become significantly more hydrophobic upon raising the temperature and, as a result, $\Delta\mu_{mic}$ and CMC become significantly lowered upon increasing T. (Jönsson et al., 1998)

5.2 CMC in surfactant mixtures

Two or more surfactants may readily mix with each other and form mixed self-assembled interfaces. The CMC in a mixture of two surfactants (denoted Surfactant 1 and Surfactant 2, respectively) is given by the following relation

$$CMC = a_1 CMC_1 + a_2 CMC_2 = \gamma_1 x CMC_1 + \gamma_2 (1-x) CMC_2 \tag{13}$$

where x is the mole fraction of Surfactant 1 *in the self-assembled interfaces*, and CMC_1 and CMC_2 are the CMCs of pure Surfactant 1 and 2, respectively. $a_1 \equiv x\gamma_1$ and $a_2 \equiv (1 - x)\gamma_2$ denote the activities of Surfactant 1 and 2, respectively, where γ_1 and γ_2 are the corresponding activity coefficients. In a surfactant mixture close to CMC it is crucial to distinguish between the mole fraction in the self-assembled interfaces (x) and the mole fraction based on the total surfactant concentration (y), including surfactant present as free monomers. It is straightforward to demonstrate that, in the limit of zero aggregate concentration, CMC as a function of y may be written as (Clint, 1975; Bergström & Eriksson, 2000)

$$\frac{1}{CMC} = \frac{y}{\gamma_1 CMC_1} + \frac{1-y}{\gamma_2 CMC_2} \tag{14}$$

The activity coefficients may be calculated from the dependence of $\Delta\mu_{mic}$ on aggregate composition employing the following expressions (Bergström & Eriksson, 2000)

$$\gamma_1(x) = \exp\left[\left(\mu_{ex}(x) - \mu_{ex}(x=1) + (1-x)\frac{d\mu_{ex}}{dx}(x'=x)\right)/kT\right] \tag{15}$$

$$\gamma_2(x) = \exp\left[\left(\mu_{ex}(x) - \mu_{ex}(x=0) - x\frac{d\mu_{ex}}{dx'}(x'=x)\right)/kT\right] \tag{16}$$

where the excess free energy per aggregated molecule is defined as

$$\mu_{ex} \equiv \Delta\mu_{mic} - kT\left[x\ln x + (1-x)\ln(1-x)\right] \tag{17}$$

Note that x in Eqs. (15) and (16) refers to the equilibrium mole fraction which is obtained by means of minimizing the molecular free energy with respect to the aggregate mole fraction x'. It follows from Eqs. (15) and (16) that a linear expression of $\mu_{ex}(x)$ gives $\gamma_1 = \gamma_2 = 1$ and, as a result, a linear (ideal) behaviour of *CMC* as a function of x.

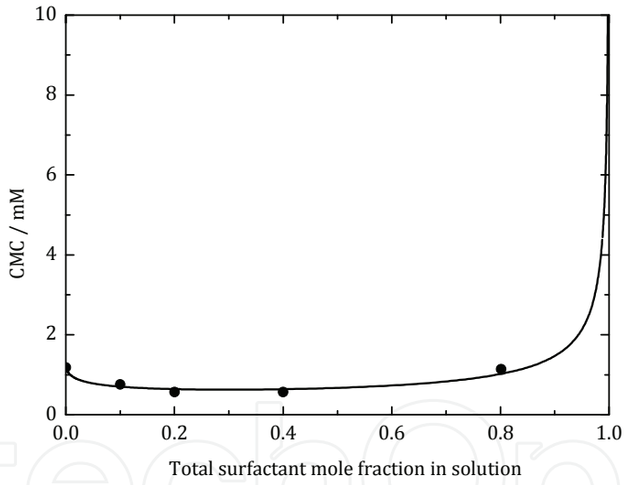

Fig. 2. The critical micelle concentration (*CMC*) plotted against the mole fraction of cationic surfactant in solution (y). The symbols represent experimentally measured values for the system sodium dodecyl sulphate (anionic surfactant)/tetracaine (cationic surfactant) in [NaCl] = 0.154 M, whereas the solid line represents calculations using the Poisson-Boltzmann theory. (Bergström & Bramer, 2008)

An ideal behaviour has usually been observed in mixtures of two rather similar surfactants, e.g. mixtures of two nonionic surfactants. On the other hand, synergistic effects, i.e. negative deviations of CMC from ideal behaviour, is frequently observed in different surfactant mixtures including ionic surfactants, for instance mixtures of an ionic and a nonionic surfactant, two oppositely charged surfactants or two surfactants with identical charge number but different tail lengths. Calculations of γ_1 and γ_2 using the Poisson Boltzmann

theory usually gives accurate agreement with experiments for these cases [*cf.* Fig. 2]. (Bergström, 2001a; Bergström et al., 2003; Bergström & Bramer, 2008)
The magnitude of synergistic or antagonistic (= positive deviation from ideal behaviour) effects may be appropriately quantified with the model-independent thermodynamic synergy parameter defined as

$$\beta_{syn} \equiv 4\ln\left(a_1 + a_2\right) = 4\ln\left(x\gamma_1 + \left(1-x\right)\gamma_2\right) \tag{18}$$

$\beta_{syn} < 0$ corresponds to a negative deviation (synergism), whereas $\beta_{syn} > 0$ implies a positive deviation (antagonism) from ideal behaviour ($\beta_{syn} = 0$). β_{syn} may be calculated from experimentally obtained *CMC* values using the relations $a_1 \equiv x\gamma_1 = y\ CMC/CMC_1$ and $a_2 \equiv (1 - x)\gamma_2 = (1 - y)\ CMC/CMC_2$ for the activities. (Bergström et al., 2003)

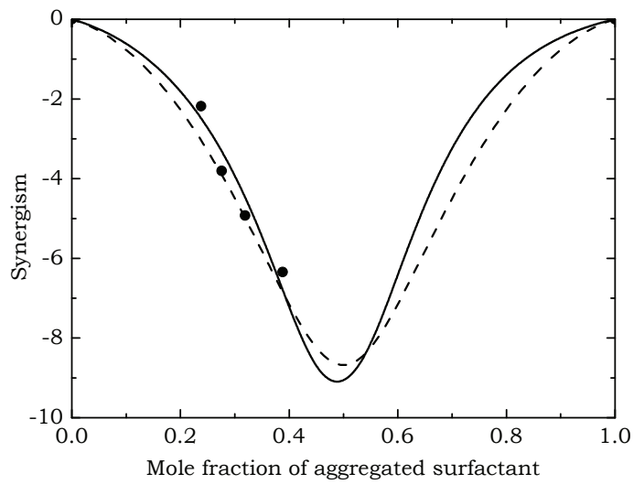

Fig. 3. The synergy parameter β_{syn} plotted against the mole fraction of self-assembled cationic surfactant (x). The symbols represent experimentally measured values for the system sodium dodecyl sulphate (anionic surfactant)/tetracaine (cationic surfactant) in [NaCl] = 0.154 M whereas the solid line is calculated from the Poisson-Boltzmann theory. The minimum is located at $x = 0.488$ where $\beta_{syn}^{min} = -9.1$. The dashed line represents the best available fit to the data obtained with the regular mixture theory giving $\beta_{syn}^{min} = \beta_{\mathrm{int}} = -8.7$. (Bergström & Bramer, 2008)

It is common to employ the theory of regular mixtures in the evaluation of CMC data for mixed surfactant systems, and quantify synergistic effects with the model-dependent interaction parameter β_{int}. (Holland, 1992) The theory of regular mixtures is based on the difference in 1-1, 2-2 and 1-2 pair-wise molecular interactions, and the corresponding excess free energy per aggregated molecule equals

$$\frac{\mu_{ex}}{kT} = \beta_{int} x\left(1-x\right) \tag{19}$$

Inserting Eq. (19) in Eqs. (15) and (16) gives $\gamma_1 = e^{(1-x)^2 \beta_{int}}$ and $\gamma_2 = e^{x^2 \beta_{int}}$. Hence, $\beta_{syn} = 4\ln\left(xe^{(1-x)^2 \beta_{int}} + (1-x)e^{x^2 \beta_{int}}\right)$, according to the regular mixture theory, always goes through a minimum at $\beta_{syn}(x = 0.5) = \beta_{int}$ (or maximum if $\beta_{int} > 0$) [cf. Fig. 3]. As a matter of fact, the factor 4 in Eq. (18) is introduced with the purpose of achieving $\beta_{syn}^{min} = \beta_{int}$ in the particular case of the regular mixture theory. However, experimentally obtained β_{syn} vs. x usually display a minimum not located at $x = 0.5$, most evident in the cases of ionic/nonionic surfactant mixtures and ionic/ionic surfactant mixtures with equal charge numbers. (Bergström et al., 2003) An exception is mixtures of two oppositely charged surfactants with equal magnitude of charge number, for which both Poisson-Boltzmann theory and regular mixture theory predicts β_{syn} to have a minimum close to (or exactly for latter case) $x = 0.5$ [cf. Fig. 3].

According to the regular mixture interpretation of deviations from ideal behaviour, favourable 1-2 interactions (as compared to 1-1 and 2-2 interactions) would cause synergism whereas unfavourable 1-2 interactions would yield antagonism. This interpretation is in sharp contrast to the thermodynamic interpretation based on Poisson-Boltzmann mean field calculations. According to the latter, synergism arises with necessity as long as two surfactants mix readily in the self-assembled interfaces and there is a pronounced asymmetry between the two surfactants. For the particular case of monovalent and oppositely charged surfactants, the asymmetry (difference in charge number = 1 – (–1) = 2) results in a release of a pair of counter-ions for every pair of surfactants that is aggregated. As a result, the chemical potential is considerably reduced and so is CMC. On the other hand, antagonism appears as a result of the surfactants not mixing properly with each other. For instance, in the extreme case where two surfactants do not mix at all and form separate one-component self-assembled interfaces, $a_1 = a_2 = 1$ which implies that $\beta_{syn} = 4\ln 2 \approx 2.77 > 0$.

6. Size distribution of self-assembled interfaces

It appears to be convenient to introduce the free energy function (Eriksson et al., 1985)

$$\mathrm{E}_N \equiv N\left(\Delta\mu_{mic} - kT\ln\phi_{free}\right) \tag{20}$$

which allows us to rewrite the set of equilibrium conditions in Eq. (8) in the following way

$$\Delta G_{tot} = \mathrm{E}_N + kT\ln\phi_N = 0 \tag{21}$$

E_N may be interpreted as the free energy of forming a self-assembled interface out of N free surfactant molecules in the bulk solution. As previously discussed, the last term in Eq. (20), including ϕ_{free}, is virtually constant above CMC. Solving ϕ_N in Eq. (21) gives the following size distribution function of self-assembled interfaces

$$\phi_N = e^{-\mathrm{E}_N/kT} \tag{22}$$

Now it is straightforward to obtain a relation between the total volume fraction of self-assembled interfaces or micelles (ϕ_{mic}) and E_N by means of summing up ϕ_N over all N, i.e.

$$\phi_{mic} = \sum_{N=1}^{\infty} \phi_N \int_1^{\infty} e^{-E_N/kT} dN \tag{23}$$

where an integral approximation have been employed in the second equality. (Israelachvili et al., 1976; Eriksson et al., 1985) From Eq. (23) it is, in principle, possible to obtain the full size distribution for an arbitrarily shaped self-assembled interface, once the mathematical form of E_N as a function of aggregate size and shape is known.

7. Bending elasticity and curvature energy

In recent years it has become widely accepted that bending properties play a decisive role as to rationalize the behaviour of self-assembled interfaces. According to the mathematical discipline of differential geometry, the curvature at a single point on a self-assembled interface (most conveniently defined at the hydrocarbon/water interface) may be defined by considering two perpendicular curves on the interface with radii of curvature, R_1 and R_2, respectively. As a result, each point at the aggregate interface may be distinguished by two principal curvatures, $c_1 \equiv 1/R_1$ and $c_2 \equiv 1/R_2$. It is postulated that the free energy per unit area γ depends uniquely on c_1 and c_2 for a given system of surfactant and solvent at some environmental condition. Moreover, by switching variables from c_1 and c_2 to the mean curvature $H \equiv \frac{1}{2}(c_1 + c_2)$ and Gaussian curvature $K \equiv c_1 c_2$, respectively, we may introduce the function $\gamma(H, K)$. (Porte, 1992; Hyde et al., 1997)

A quantitative description of the bending properties of self-assembled interfaces is obtained as γ is expanded to second order with respect to H and K, i.e.

$$\gamma(H,K) = \gamma_0 + 2k_c (H - H_0)^2 + \bar{k}_c K \tag{24}$$

commonly referred as to the Helfrich expression. (Helfrich, 1973) The total free energy of a self-assembled interface, corresponding to the E_N-function defined in Eq. (20), is given as an integral of γ over the entire interfacial area A of the self-assembled interface, i.e.

$$E_N = \int \gamma(H,K) dA = \gamma_0 A + 2k_c \int (H - H_0)^2 dA + \bar{k}_c \int K dA \tag{25}$$

The first term on the right-hand side of Eq. (25) (= $\gamma_0 A$) represents the free energy of stretching the self-assembled interface. The second and third terms take into account effects due to the dependence of free energy on the local curvature of the self-assembled interface, usually referred as to the bending free energy.

The Helfrich expression introduces three important parameters related to different aspects of bending a surfactant monolayer interface, i.e. the bending rigidity (k_c), the spontaneous curvature (H_0) and the saddle splay constant ($\bar{k}_c$). As a common notation, we will refer to all of them below as bending elasticity constants. For thermodynamically stable objects, such as surfactant micelles and bilayers, the three bending elasticity constants may be interpreted as thermodynamic parameters, and they may be calculated from any suitable molecular model by means of minimizing the free energy per molecule of a surfactant interfacial layer at any given H and K. (Bergström, 2006a; Bergström, 2006b; Bergström, 2008a).

7.1 Bending rigidity

The bending rigidity k_c quantifies the resistance against deviations from a uniform mean curvature $H = H_0$. Positive values of k_c secures $\gamma(H, K)$ to display a minimum with respect to H, whereas negative k_c -values corresponds to γ having a maximum. As a consequence, the sign of k_c determines the stability of an amphiphilic self-assembled interface, i.e. stable interfaces may only exist for positive values of k_c. Moreover, high k_c -values are expected to favour self-assembled interfaces with small deviations from a homogenous curvature or geometry, i.e. rigid and monodisperse objects with a uniform shape [see further below]. (Porte, 1992; Bergström, 2007; Bergström, 2008a)

From a molecular point of view, k_c appears to be a measure of the amphiphilic nature of a surfactant molecule, and it displays a clear maximum when plotted against the ratio between the hydrophilic and hydrophobic (= lipophilic) parts, respectively, of an amphiphilic molecule. This maximum corresponds to the optimal hydrophilic-lipophilic balance (HLB) of a surfactant molecule [*cf.* Fig. 4]. (Bergström, 2009) For instance, attaching a point charge to the end of a C_{12} aliphatic hydrocarbon chain significantly rises k_c to positive values as the molecule become amphiphilic in nature. (Bergström, 2006a) On the other hand, if either the hydrophilic or the hydrophobic part of the molecule becomes too large or small compared to the other, k_c may become negative which means that the amphiphilic nature of the molecule is too weak for stable surfactant self-assembled interfaces to form.

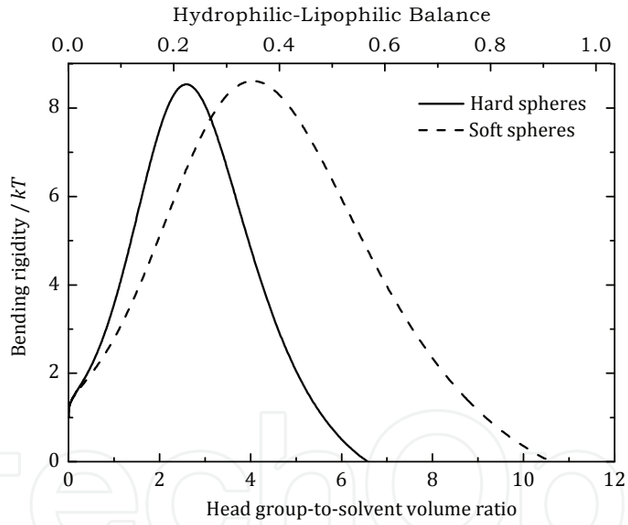

Fig. 4. Bending rigidity (k_c) plotted against the head group-to-solvent volume ratio and the hydrophilic-lipophilic balance (HLB) for a self-assembled interface formed by a single-chain nonionic surfactant with the head group treated as a hard sphere (solid line) and a soft sphere (dashed line), respectively. (Bergström, 2009)

The flexibility of surfactant tails appears to be crucial for the self-assembly process of nonionic surfactants. In accordance, it may be demonstrated that k_c must always equal zero, thus preventing self-assembly, for nonionic surfactants made up of a hydrophobic and a hydrophilic part that are both rigid. (Bergström, 2009) Ionic surfactants with a rigid hydrophobic part may have $k_c > 0$, but are predicted to behave substantially different than conventional ionic surfactants. With comparatively small k_c and high $k_c H_0$, they appear to be

much smaller and more polydisperse than micelles formed by an ionic surfactant with flexible tail. (Bergström, 2006a)

Moreover, in expressions derived for k_c as a function of composition in a surfactant mixture, an explicit contribution appears that is due to the mixing of surfactants in the self-assemblies *per se*. (Kozlov & Helfrich, 1992; Porte & Ligoure, 1995; Safran, 1999; Bergström, 2006b) This contribution always brings down k_c, and the magnitude of this reduction increases with increasing asymmetry between two surfactants with respect to head group charge number, volume of surfactant tail etc. The origin of this mixing dependence of k_c is as follows: the surfactant composition, as obtained by minimizing the molecular free energy at given H and K, becomes a smooth function of aggregate curvature. As a consequence, different geometrical parts of a self-assembled interface may have different surfactant compositions so as to enrich the surfactant (in an aqueous solvent) with the highest HLB in the most curved parts of the interface. As a result, the free energy penalty of distorting the aggregate curvature from its optimal value (= H_0) becomes significantly reduced as k_c decreases in magnitude upon mixing. Corresponding explicit dependences on mixing are absent for the other two bending elasticity constants, i.e. k_cH_0 and $\bar{k}_c$.

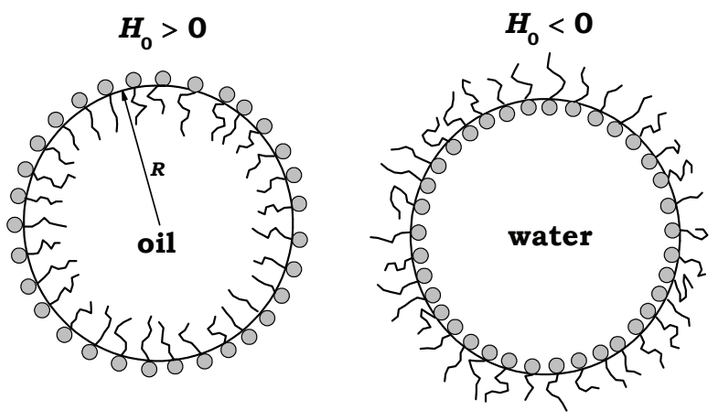

Fig. 5. Schematic illustration of a spherical oil-in-water and water-in-oil microemulsion droplet, respectively, with radius R. (Bergström, 2008a)

7.2 Spontaneous curvature

The spontaneous curvature H_0 represents the sign and magnitude of the preferential curvature of a single surfactant layer. H_0 is usually defined to be positive for a film that appears convexly curved from a position in the hydrophilic phase, like ordinary surfactant micelles in water or oil-in-water microemulsion droplets [*cf.* Fig. 5]. As a matter of fact, it appears that the product k_cH_0 is more readily to interpret from a physical and molecular point of view than H_0 itself. k_cH_0 depends on the architecture of an amphiphilic molecule in such a way that it increases with increasing hydrophilic-lipophilic balance [*cf.* Fig 6]. (Bergström, 2006a; Bergström, 2009) As a result, k_cH_0 rapidly decreases with increasing surfactant tail length whereas ionic surfactants usually have larger k_cH_0 than nonionic surfactants. Consequently, as an additional oil phase of solvent is present, surfactants with a high HLB tends to form oil-in-water microemulsion droplets whereas surfactants with low HLB values tend to form water-in-oil droplets [*cf.* Fig. 5].

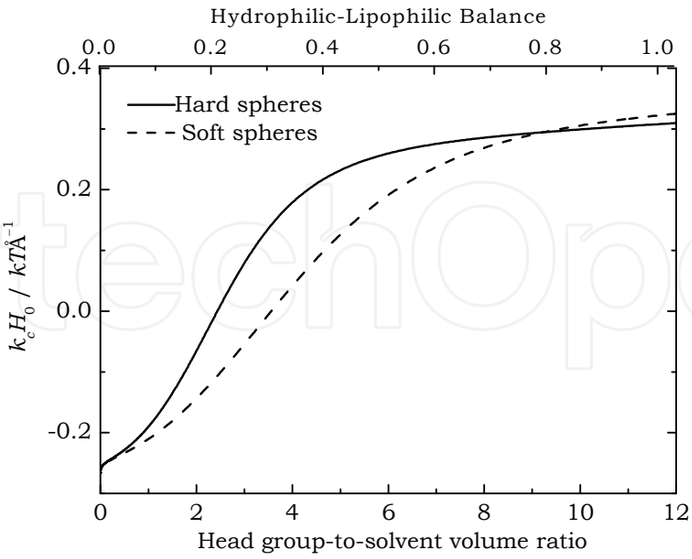

Fig. 6. Bending rigidity times the spontaneous curvature (k_cH_0) plotted against the head group-to-solvent volume ratio and the hydrophilic-lipophilic balance (HLB) for a self-assembled interface formed by a single-chain nonionic surfactant with the head group treated as a hard sphere (solid line) and a soft sphere (dashed line), respectively. (Bergström, 2009)

7.3 Saddle-splay constant

All interfacial shapes that may be generated from one another by twisting and stretching, without breaking the interface, belong to the same topology. (Hyde et al., 1997) Different topologies are characterized with the quantity genus (g), which represents the number of handles or holes present in the self-associated interface. For instance, ordinary surfactant micelles may be spherical, cylindrical or tablet-shaped (see further below) but belong to the same topology since the self-assembled interfacial layer is geometrically closed ($g = 0$).
According to the so called Gauss-Bonnet theorem,

$$\int K dA = 4\pi(1-g) \tag{26}$$

As a result, the last term in Eq. (25), for a geometrically closed interface ($g = 0$), equals $4\pi\bar{k}_c$, the quantity of which does not depend on the size of the self-assembled interface. Since $\bar{k}_c$ contributes with a size-independent term to E_N, the value of $\bar{k}_c$ indirectly determines the size of a dispersed set of geometrically closed self-assembled interfaces. Positive values of $\bar{k}_c$ means that the total free energy in the system increases as one single self-assembled interface is split up to form two or many smaller interfaces. As a result, increasing values of $\bar{k}_c$ favours large aggregation numbers. Calculations based on detailed molecular models indicate that $\bar{k}_c$ usually assumes negative values, favouring the formation of small self-assembled interfaces. (Bergström, 2006a; Bergström, 2009).
It has been demonstrated that the remaining parameter in Eqs. (24) and (25), the interfacial tension γ_0, is directly determined for a given concentration of micelles ϕ_{mic}. (Israelachvili et

al., 1976; Bergström, 2006c) As a consequence, it follows that the overall average size in a dispersion of self-assembled interfaces is determined by, in addition to the three bending elasticity constants, the total surfactant concentration ($\phi_{tot} = \phi_{mic} + \phi_{free}$). This dependence is a result of the entropy of self-assembly which, according to Eqs. (3) and (4), effectively works as a driving force tending to reduce the size of self-assembled interfaces. This effective driving force increases in magnitude with decreasing surfactant concentration and, as a consequence, surfactant micelles are occasionally find to increase in size with increasing surfactant concentration [see further below].

8. Spherical micelles and microemulsion droplets

The simplest geometry of a self-associated surfactant monolayer interface is the geometrically closed spherical shape. This is the only geometrical shape for which the curvature is equal on every single point on the self-assembled interface. The free energy as a function of the radial distance to the hydrophobic-hydrophilic interface (R), in accordance with Eq. (25), is simply obtained by inserting $c_1 = c_2 = 1/R$ in the Helfrich expression in Eq. (24) and multiplying γ with the surface area $A = 4\pi R^2$. (Safran, 1991; Bergström, 2008a).

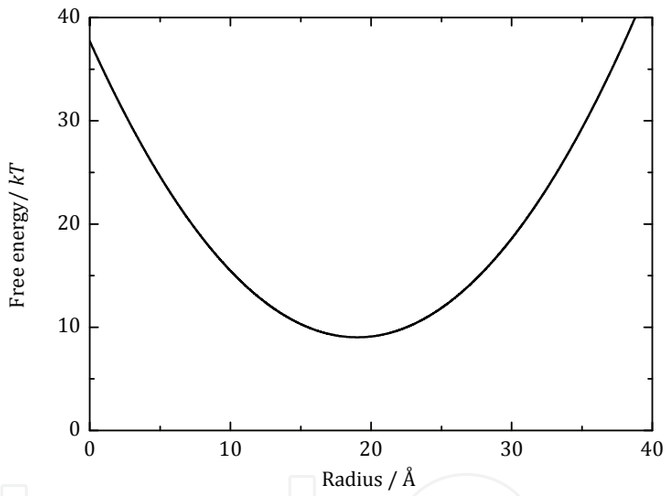

Fig. 7. The free energy E of spherical micelles as a function of radius R for the case of bending elasticity constants set to $H_0 = 0.03$ Å^{-1}, $k_c = 2kT$ and $\bar{k}_c = -kT$

As a result,

$$\mathrm{E}(R) = 4\pi\left(2k_c + \bar{k}_c - 4k_c H_0 R + \gamma_p R^2\right) \tag{27}$$

where $\gamma_p \equiv \gamma\left(H = K = 0\right) = \gamma_0 + 2k_c H_0^2$ is the interfacial tension of a strictly planar surfactant layer. Hence, E may be considered as the sum of two contributions: (*i*) the stretching work of forming a planar interface [$= 4\pi R^2 \gamma_p$] and (*ii*) the work of bending the interface at constant interfacial area [$= 4\pi\left(2k_c + \bar{k}_c - 4k_c H_0 R\right)$].

Eq. (27) is plotted in Fig. 7 for a set of typical values of the bending elasticity constants. It follows from Eq. (27) that the free energy of a spherical micelle is proportional to the

aggregation number N in the limit $N \to \infty$, consistent with the thermodynamics of large macroscopic systems. In our treatment, however, it has become clear that non-extensive contributions to E(R) appear as a result of curvature effects and, as a consequence, a sharp minimum of E(R) is observed in Fig. 7, the location of which is mainly determined by the spontaneous curvature. The appearance of significant non-extensive contributions to the free energy is the basis of the discipline called thermodynamics of small systems. (Hill, 1963-64)

8.1 Size distribution of spherical micelles and microemulsion droplets

The size distribution of spherical micelles may be obtained by inserting Eq. (27) in Eq. (23) and switching variables in accordance with $dN = 4\pi R^2 dR/v$, where v is the molecular volume of the surfactant. As a result,

$$\phi_{mic} = \int_0^\infty \phi(R)\,dR = \int_0^\infty \frac{4\pi R^2}{v} e^{-4\pi\left(2k_c + \bar{k}_c - 4k_c H_0 R + \gamma_p R^2\right)/kT} dR \tag{28}$$

The volume fraction density $\phi(R)$ according to Eq. (28) is plotted in Fig 8. The size distribution function appears to be close to Gaussian with a sharp peak located at the minimum of E(R).

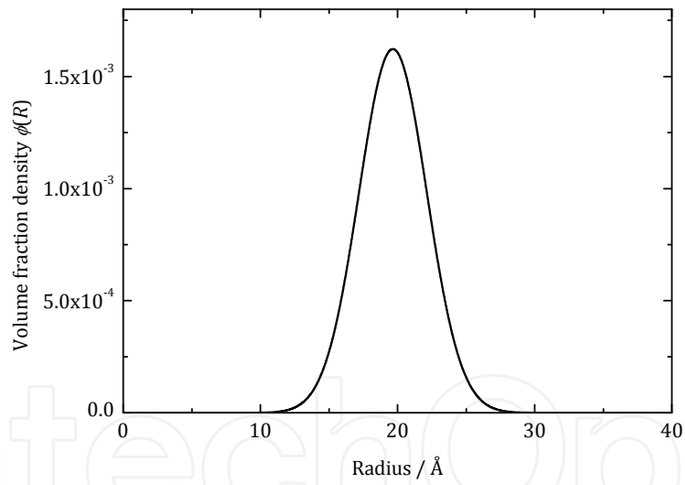

Fig. 8. Size distribution of spherical micelles for the case of bending elasticity constants set to $H_0 = 0.03$ Å^{-1}, $k_c = 2kT$ and $\bar{k}_c = -kT$

The size distribution shown in Fig. 8 is obtained by giving the spontaneous curvature a rather large value (H_0 = 0.03 Å^{-1}), implying an average micelle radius $\langle R \rangle \approx 20$ Å. This is about the largest accessible value for micelles made up of surfactants with a C_{12} aliphatic chain to retain a strictly spherical shape. Upon further decreasing H_0, the micelles tend to grow in size so as to achieve a reduced interfacial curvature. However, at some point the micelle radius starts to exceed the length of a fully stretched surfactant molecule and, in order to avoid the formation of a hole in the centre of the hydrophobic micelle core, surfactant micelles must assume some kind of non-spherical shape. Non-spherical micelles

will be treated below in Section 9. Alternatively, in systems including, in addition to surfactant and water, a hydrophobic component (oil), the micelle core may be filled up with oil molecules to retain its spherical shape [*cf.* Fig 5].

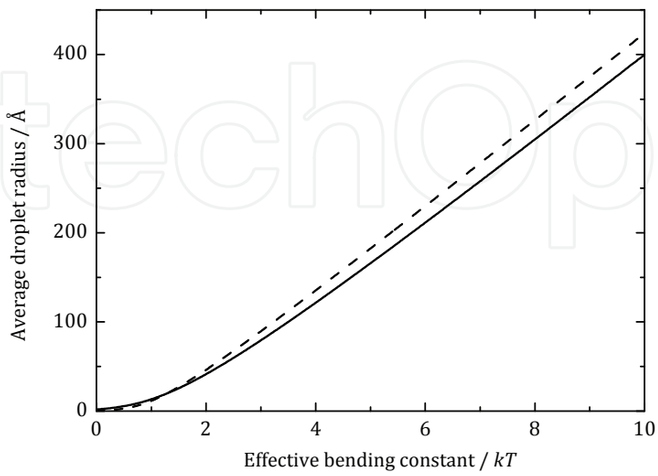

Fig. 9. The volume equivalent average droplet radius $\langle R \rangle$ for an ellipsoidal microemulsion droplet (solid line) and for a strictly spherical droplet (dashed line) plotted against the effective bending constant $k_{eff} \equiv 2k_c + \bar{k}_c$ for given values of $H_0 = 0.01$ Å^{-1} and $k_c = kT$. (Bergström, 2008a)

An explicit expression for the average size of a spherical micelle or microemulsion droplet may be derived from a given size distribution function as

$$\langle R \rangle = \frac{1}{\phi_{mic}} \int_0^\infty R\phi(R)\,dR \tag{29}$$

As a result, we obtain (Bergström, 2008a)

$$\langle R \rangle = H_0^{-1} \left(1 + \frac{\bar{k}_c + k_S}{2k_c} \right) \frac{1}{f(z)} \tag{30}$$

where $f(z)$ is a function that approaches zero as $z \to 0$ and equals unity as $z \to \infty$ and

$$z \equiv \frac{16\pi (k_c H_0)^2}{\gamma_p kT} = \frac{4\pi}{kT} \left(2k_c + \bar{k}_c + k_S \right) \tag{31}$$

The exact appearance of $f(z)$ depends on in what way shape fluctuations of the droplets are taken into account. k_S is a parameter, in units of energy, that takes into account the unfavourable entropy of self-assembling surfactant molecules in micelles (or surfactant and oil molecules in microemulsion droplets). k_S assumes negative values and equals zero as $N \to 1$ (equivalent to $k_{eff} \equiv 2k_c + \bar{k}_c \to 0$, *cf.* Fig. 9). $f(z) = 1$ whereas k_S becomes constant in the limit of large values of the effective bending constant ($k_{eff} \equiv 2k_c + \bar{k}_c$).

The average radius of swollen micelles and microemulsion droplets as a function of the effective bending constant k_{eff}, in accordance with Eq. (30), is plotted in Fig. 9. It appears that the droplet radius always vanishes in the limit $k_{eff} \to 0$. This is a general feature that emphasizes k_{eff} as a direct measure of the strength of the driving force of self-assembling amphiphilic molecules, the criterion of which is $k_{eff} > 0$. As k_{eff} turns into negative values, the hydrophobic driving force is no longer strong enough so as to counteract the entropy of self-assembly, and the surfactant is expected to be present as free molecules.

It is evident that all bending elasticity constants, as well as k_S, contribute to the final size of spherical micelles or microemulsion droplets. The droplet size is directly influenced by H_0, $\bar{k}_c$ and k_S. $\langle R \rangle$ increases as the curvature of the droplets tends to decrease with decreasing H_0, whereas the droplet size increases with increasing $\bar{k}_c$ as a result of the Gauss-Bonnet theorem discussed above. (Safran, 1991) Self-association entropy effects, taken into account by $k_S < 0$, tend to decrease the size of the micelles and droplets as it becomes increasingly more unfavourable to self-assemble surfactant and solute molecules with increasing aggregation number N. (Bergström, 2008a).

The bending rigidity influences $\langle R \rangle$ in a more indirect way. At high k_c -values, the influences of $\bar{k}_c$ and k_S are reduced since the free energy penalty to change the interfacial curvature from a uniform value equal to H_0 is large, and $\langle R \rangle \approx 1 / H_0$. On the other hand, lowering k_c is expected to increase the magnitude of deviations from a spontaneous curvature. Since both $\bar{k}_c$ and k_S are usually negative, the droplet size is usually found in the regime $\langle R \rangle < 1 / H_0$.

The polydispersiy, in terms of the relative standard deviation, is defined as

$$\frac{\sigma_R}{R} = \sqrt{\frac{\langle R^2 \rangle}{\langle R \rangle^2} - 1} \tag{32}$$

and it may be evaluated for spherical micelles and microemulsion droplets employing the size distribution function in Eq. (28) [*cf.* Fig. 10]. It is seen that as $k_{eff} \to 0$, $\sigma_R / \langle R \rangle$ approaches a constant value that depends on how shape fluctuations are taken into account. As $k_{eff} \to \infty$, the polydispersity approaches the expression (Safran, 1991; Bergström, 2008a)

$$\frac{\sigma_R}{R} = \sqrt{\frac{kT}{8\pi\left(2k_c + \bar{k}_c + k_S\right)}} \tag{33}$$

Hence, the polydispersity appears to be a function of mainly k_{eff}. $\sigma_R / \langle R \rangle$ is primarily influenced by the bending rigidity since low values of k_c allows for large variations in droplet curvature. However, $\sigma_R / \langle R \rangle$ is also indirectly influenced by $\bar{k}_c$ through a constraint of fixed surfactant and oil concentration. The number of droplets must always increase with increasing polydispersity for a given droplet volume fraction and, as a consequence, the droplet polydispersity becomes raised as $\bar{k}_c$ is decreased. (Safran, 1991) Eqs. (30) and (33) have been derived by Safran for the case where self-association entropy effects have been neglected, i.e. with $f(z) = 1$ and $k_s = 0$ [*cf.* Fig. 10]. (Safran, 1991).

Finally, allowing for ellipsoidal shape fluctuations of micelles or droplets it may be demonstrated that deviations from a spherical shape increase with decreasing values of k_c, whereas the droplet shape is not influenced by $k_c H_0$ and $\bar{k}_c$ [*cf.* Fig 11]. (Bergström, 2008a).

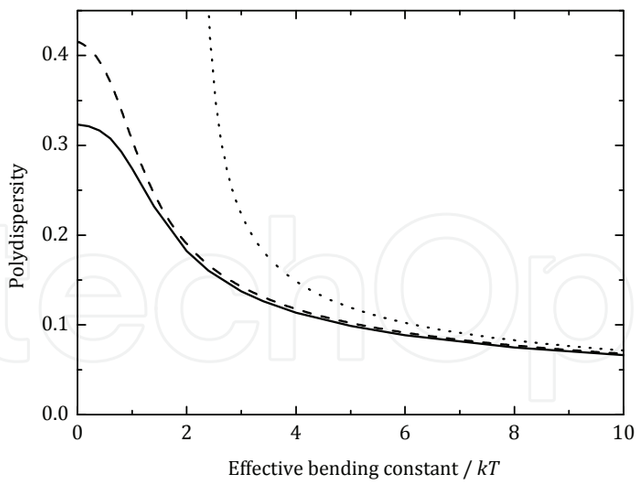

Fig. 10. The polydispersity $\sigma_R/\langle R\rangle$ of ellipsoidal microemulsion droplets (solid line) and strictly spherical droplets (dashed line) plotted against the effective monolayer bending constant $k_{eff} \equiv 2k_c + \overline{k}_c$. The dotted line represents $\sigma_R/\langle R\rangle$ as calculated from Eq. (30) with $f(z) = 1$ and $k_s = 0$. (Bergström, 2008a)

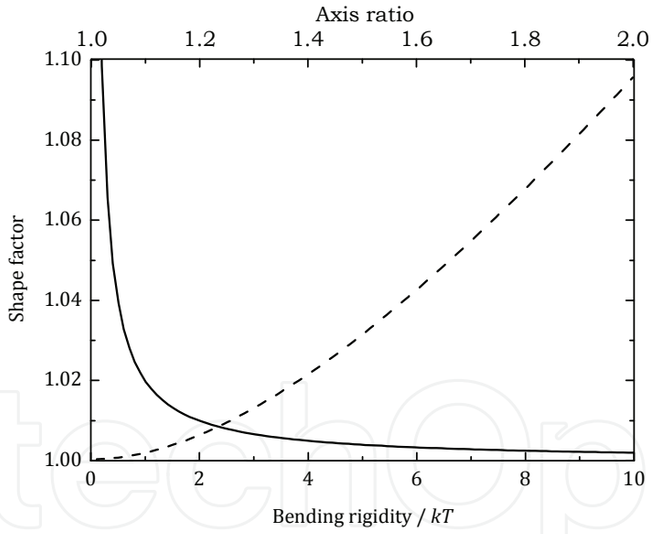

Fig. 11. The average shape factor $\langle\chi\rangle \equiv \langle A\rangle/4\pi R^2$ for ellipsoidal microemulsion droplets plotted against the bending rigidity k_c (solid line, bottom axis) for given values of $H_0 = 0.01$ Å^{-1} and $\overline{k}_c = 0$. The dashed line shows χ as a function of the axial ratio ε (top axis). (Bergström, 2008a)

9. Non-spherical micelles

In a solution with only surfactant and water present (and no oil), the strictly spherical shape of micelles corresponds to a minimum in size. As already mentioned, as micelles grow beyond a certain aggregation number they are forced to turn into some kind of non-spherical shape. As

a result, they may grow in length to become shaped as long rods, worms or threads. Alternatively, they may grow both with respect to length and width to form disklike micelles or some kind of bilayer structure [see Section 10 below]. The thickness, however, must be more or less constant, approximately equalling twice the length of a surfactant molecule. The most general form of a growing surfactant micelle is the so called tablet-shaped or triaxial micelle. The tablet is characterized as having three dimensions (thickness, width and length) that may be different from one another. An example is the triaxial ellipsoid, the model of which has proven to be able to accurately fit small-angle scattering data of surfactant micelles. (Bergström & Pedersen, 1999a; Bergström & Pedersen, 1999b).

9.1 Tablet-shaped micelles

In order to investigate the influence of the various bending elasticity constants on the width and length of a tablet-shaped micelle, a theoretical model has recently been developed. (Bergström, 2007) In this model a tablet-shaped micelle is considered as composed of three geometrical parts: (*i*) a central planar bilayer surrounded by (*ii*) two straight semi-cylindrical rims and (*iii*) two semi-toroidal rims [*cf.* Fig. 12]. The planar bilayer is composed of a rectangular part with length L and width $2R$ with two semi-circular parts with radius R at each short side. The thickness of the bilayer part equals 2ξ and the radii of the cylindrical and toroidal rims equal ξ.

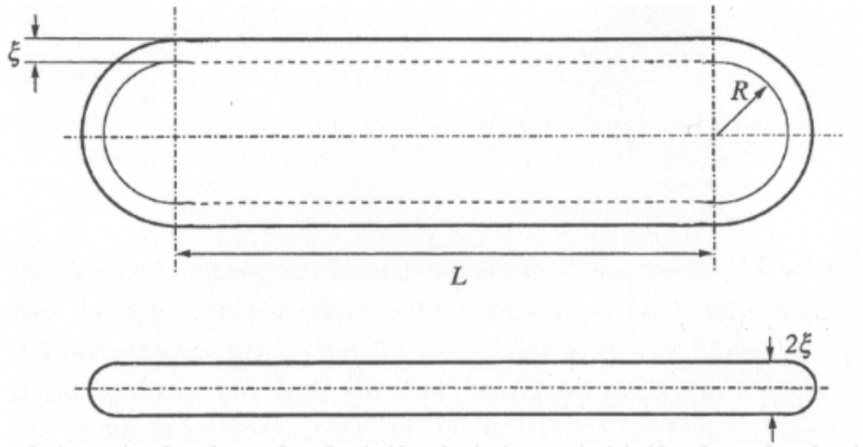

Fig. 12. Schematic illustration of a tablet-shaped micelle. (Bergström, 2007)

The free energy of a tablet-shaped micelle as a function of the dimensionless half width ($r \equiv R/\xi$) and the dimensionless length of the central bilayer part ($l \equiv L/\xi$) have been derived from Eq. (25) giving

$$\frac{\mathrm{E}(r,l)}{kT} = \alpha + \delta\psi(r)\beta(\pi r + l) + 2r(\pi r + 2l)\lambda \tag{34}$$

where the reduced planar interfacial tension is defined as $\lambda \equiv \xi^2\gamma_p / kT$ and $\alpha \equiv 2\pi\left(3k_c + 2\bar{k}_c - 8\xi k_c H_0\right)/kT + 4\pi\lambda$, $\beta \equiv \pi k_c(1 - 4\xi H_0)/kT + 2\pi\lambda$ and $\delta \equiv 2\pi k_c / kT$ are three dimensionless parameters taking into account the bending free energy. The ψ-function ($0 < \psi < 1$) equals unity in the limit $r \to 0$ and zero as $r \to \infty$. (Bergström, 2007; Bergström, 2008b).

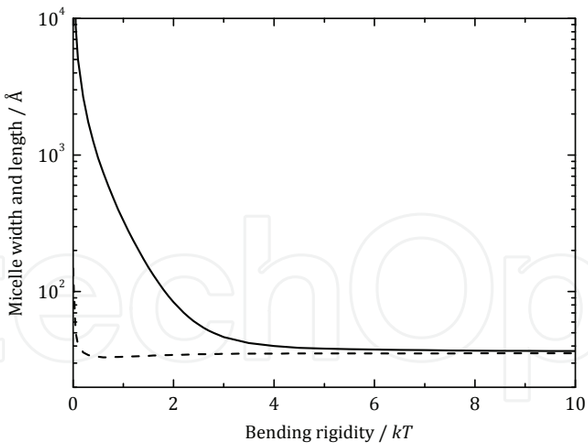

Fig. 13. The average length ⟨Λ⟩ (solid line) and width ⟨Ω⟩ (dashed line) of tablet-shaped micelles plotted against the bending rigidity. The spontaneous curvature was set to $H_0 = 1/2\xi$ with $\xi = 12$ Å. β was set equal to zero corresponding to the maximum attainable size of the micelles. (Bergström, 2007)

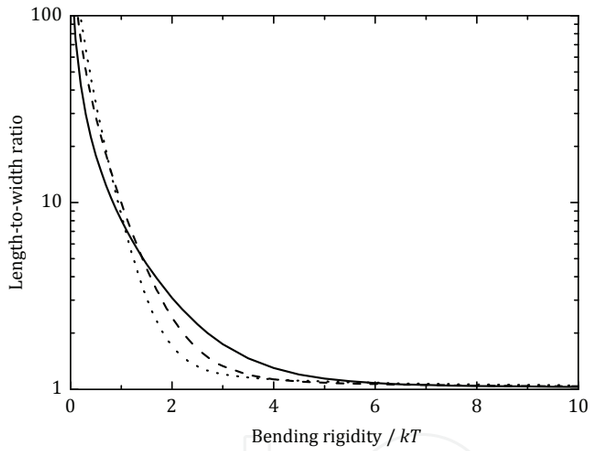

Fig. 14. The length-to-width ratio ⟨Λ⟩/⟨Ω⟩ of tablet-shaped micelles plotted against the bending rigidity. The spontaneous curvature was set to $H_0 = 1/\xi$ (solid line), $H_0 = 1/2\xi$ (dashed line) and $H_0 = 1/3\xi$ (dotted line) with $\xi = 12$ Å. β was set equal to zero corresponding to the maximum attainable size of the micelles. (Bergström, 2007)

The corresponding size distribution of tablet-shaped micelles has been evaluated by inserting Eq. (34) in Eq. (23). As a result, by means of integrating over l the following relation is obtained

$$\phi_{mic} = \frac{\pi\xi^6}{v^2}\int_0^\infty \frac{8r^2 + 6\pi r + \pi^2}{\beta + 4\lambda r} e^{-\delta\psi(r) - \pi\beta r - 2\pi\lambda r^2} dr \tag{36}$$

From the length and width distribution function it is straightforward to calculate the average width ⟨Ω⟩ ≡ 2(⟨R⟩ + ξ) and length ⟨Λ⟩ ≡ ⟨L⟩ + ⟨Ω⟩, in a dispersed phase of tablet-

shaped micelles, as functions of the different bending elasticity constants. It appears that $k_c H_0$ mainly influence the width of the micelles ($\langle\Omega\rangle$ increases slightly with decreasing $k_c H_0$) whereas the length of the micelles increase significantly upon lowering the bending rigidity. As a consequence, more disklike ($l = 0$ in Eq. (34) and Fig. 12) or oblate shaped micelles are expected at high k_c -values, whereas elongated worms or threads are expected at k_c -values below about kT [*cf.* Figs. 13 and 14]. For instance, spherocylindrical micelles (two hemispheres attached to the ends of a cylinder, $r = 0$ in Eq. (34) and Fig. 12) are expected to be present at large values of $k_c H_0$ and low k_c. This behaviour may be rationalized as a result of the property of k_c to influence to what extent self-assembled interfaces are composed of geometrical parts with different curvatures. For instance, the large difference in curvature between the cylinder and hemispherical parts of a spherocylindrical micelle is favoured by low k_c -values. The saddle-splay constant contributes with a constant factor to the micelle size distribution and influence the size of tablet-shaped micelles (including spherocylinders and disks), but not the shape.

In the extreme case of long spherocylindrical micelles, the work of inserting an extra molecule in the cylinder part of a micelle is much lower than the work (per molecule) of forming an additional micelle with an extra pair of hemispheres. As a result, all surfactant molecules that are added will be incorporated in the existing micelles and, as a consequence, the micelles grow in length with increasing surfactant concentration in accordance with $\langle L\rangle \propto \phi_{mic}$, whereas the number of micelles is not changed. (Bergström, 2001b) Likewise, the (volume-weighted) relative standard deviation reaches a maximum value of $\sigma_L/\langle L\rangle = 1$ for spherocylindrical micelles. This behaviour is in sharp contrast to what is predicted for spherical or disklike micelles that form as the bending rigidity is large in magnitude. In the latter case, the curvature of a single micelle is changed upon inserting an extra molecule and, as a result, the work of forming an extra micelle is lower than the work of inserting the same amount of molecules in the existing micelles. Hence, adding surfactant to a system of spherical or disklike micelles increases the number of micelles, but does not change the micelle size, and the micelles turn out be nearly monodisperse. As a consequence, both growth rate and polydispersity of oblong tablet-shaped micelles are predicted to increase with decreasing k_c -values so as to finally reach the maximum values of long spherocylindrical micelles.

Moreover, Eq. (36) sets the limits for the existence of a solution of thermodynamically stable tablet-shaped micelles. (Bergström, 2007) According to Eq. (36), there is a maximum value that ϕ_{mic} may attain as the parameter β approaches zero. If the concentration of self-assembled surfactant exceeds this maximum value it is required that $\beta = r = 0$ so as to fulfil the condition of constant total surfactant concentration. There is no resistance for micelles to grow in the length direction as β and r reaches zero and, as a consequence, infinitely long cylinders ($r = 0$), rather than discrete tablet-shaped micelles, are expected to form above this critical concentration of surfactant. The surfactant concentration where the transition from discrete tablets to infinite cylinders is expected to occur decreases with increasing values of the effective bending constant $k_{eff} = 2k_c + \bar{k}_c$.

9.2 Toruslike micelles

Alternatively, toruslike micelles (cylinder that is geometrically closed in a ring shape), rather than infinite cylinders, may form at large k_{eff} -values, in the regime where tablets may not

form. The free energy of toruslike micelles may be derived in a similar way as for tablets giving (Bergström, 2008b)

$$\frac{\mathrm{E}(r)}{kT} = 2\pi r\left[\beta + \frac{\pi k_c}{kT}\left(\frac{r}{\sqrt{r^2-1}} - 1\right)\right] \tag{37}$$

where $r = R/\xi$ is the dimensionless torus radius and $\beta \equiv \pi k_c\left(1 - 4\xi H_0\right)/kT + 2\pi\lambda$ is defined in the same way as for tablet-shaped micelles in Eq. (34). Toruslike micelles belong to a different topology than tablets, with a single hole and a genus $g = 1$. As a result, the integral over the Gaussian curvature in Eq. (26) equals zero and, as a consequence, $\bar{k}_c$ is absent in Eq. (37). From the Gauss-Bonnet theorem, this implies that tori are favoured at the expense of tablets by large values of the saddle-splay constant.
The size distribution function for toruslike micelles equals

$$\phi_{tor} = \frac{2\pi^2\xi^3}{v}\int_1^\infty \exp\left[-2\pi\beta r - \frac{2\pi^2 k_c}{kT} r\left(\frac{r}{\sqrt{r^2-1}} - 1\right)\right] dr \tag{38}$$

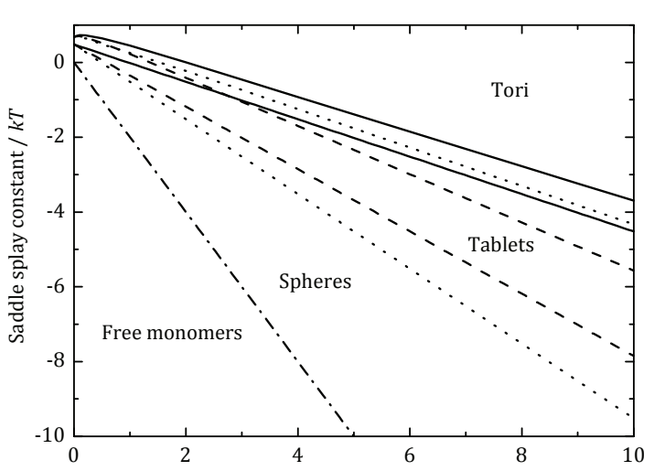

Fig. 15. Diagram showing regimes where toruslike, tablet-shaped and spherical micelles are predicted to predominate at $\xi H_0 = 1/2$ (solid lines), $\xi H_0 = 1/3$ (dashed lines) and $\xi H_0 = 1/4$ (dotted lines). Surfactants do not self-assemble in an aqueous solvent below the dash-dotted line, corresponding to $k_{eff} = 2k_c + \bar{k}_c = 0$. (Bergström, 2008b)

By setting $\phi_{mic} = \phi_{tor}$ according to Eqs. (36) and (38), we obtain the micelle predominance diagram in Fig. 15. It is seen that toruslike micelles are expected to be found at large values of k_c and $\bar{k}_c$, whereas a transition to tablets (including spherocylinders and disks) is expected as $k_{eff} = 2k_c + \bar{k}_c$ is lowered. As k_{eff} is further decreased, the tablets become smaller in size, eventually ending up as spheres. As k_{eff} falls below zero the surfactant may no longer form micelles and is expected to be present as free surfactant [*cf.* Fig. 9].
A second type of abrupt transition is predicted from Eq. (36). (Bergström, 2007) In the vicinity of $H_0 = 1/4\xi$, tablet-shaped micelles grow considerably in both width and length to

form large but discrete bilayer fragments. The width-to-length ratio is determined by the magnitude of the bending rigidity and large circular disks may be present in so far k_c is large in magnitude and $H_0 \gtrsim 1/4\xi$. As H_0 is further decreased, ϕ_{mic} rapidly approaches zero and as H_0 falls below $1/4\xi$ thermodynamically stable micelles can no longer exist. Rather than micelles, various types of bilayer structures appear to predominate as $H_0 < 1/4\xi$. A micelle-to-bilayer transition at $H_0 = 1/4\xi$ is also predicted from Eq. (38) for toruslike micelles. (Bergström, 2008b)

The behaviour of surfactant micelles as a function of the various bending elasticity constants is summarized in Table 1.

Micellar systems ($H_0 > 1/4\xi$)	Small $\bar{k}_c$	Large $\bar{k}_c$
Small k_c	Rods	Disordered Cylinders or Tori
Large k_c	Disks	Ordered Cylinders or Tori

Table 1. The structural behaviour of self-assembled micellar systems with bending rigidity and saddle-splay constant

10. Bilayers

10.1 Vesicles

As $H_0 < 1/4\xi$, amphiphilic molecules are predicted to self-assemble into various kinds of bilayer structures. In comparatively small and discrete form, bilayers tend to close themselves geometrically in order to eliminate their unfavourable edges and form vesicles (spherical bilayer shells). Vesicles may be considered as made up of an outer, positively curved ($H > 0$), and an inner, negatively curved ($H < 0$), monolayer [*cf.* Fig. 16].

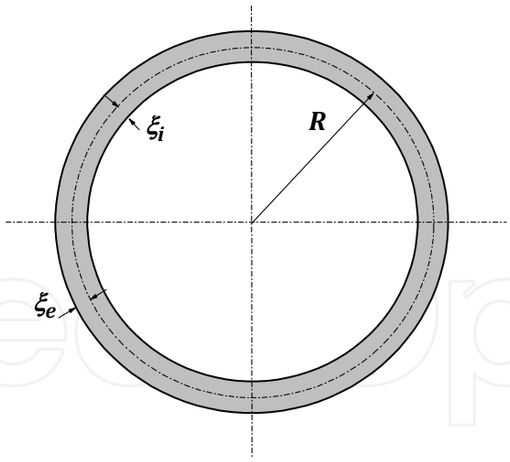

Fig. 16. Schematic representation of a unilamellar vesicle with radial distance R to the surface that divides the inner and the outer monolayers, the thicknesses of which are denoted ξ_i and ξ_e, respectively. (Bergström, 2001c)

The free energy of a vesicle may be derived in a similar way as for micelles giving (Helfrich, 1973; Bergström & Eriksson, 1996)

$$\mathrm{E}(R) = 4\pi\left(k_{bi} + 2\gamma_p R^2\right) \tag{39}$$

where the bilayer bending constant

$$k_{bi} = 4k_c\left(1 - 2\xi H_0\right) + 2\bar{k}_c \tag{40}$$

incorporates contributions due to the bending of a planar bilayer at constant interfacial area [$= 8\pi\gamma_p R^2$]. Considering the entire bilayer as a closed interface gives a topology with genus $g = 0$. However, if we want to compare with tablet-shaped ($g = 0$) and toruslike micelles ($g = 1$), we must consider each single monolayer as an interface, and the vesicle as consisting of two closed interfaces. As a result, the genus of a unilamellar vesicle equals $g = -1$ and, consequently, the integral in Eq. (26) equals 8π, and a term equal to $8\pi\bar{k}_c$ appears in Eq. (39). The size distribution of vesicles may be written as (Bergström, 2001c)

$$\phi_{ves} = const \times \int_0^\infty R^\alpha e^{-4\pi\left(k_{bi} + 2\gamma_p R^2\right)} dR \tag{41}$$

Notably, the bending free energy ($= 4\pi k_{bi}$) is constant with respect to vesicle size, implying that high values of k_{bi} favours large vesicles. This is consistent with Eq. (41), according to which the aggregation number $\langle N \rangle \propto e^{-4\pi k_{bi}}$. Hence, rather small unilamellar vesicles are expected to form at comparatively low values of k_{bi} whereas, at higher k_{bi}, the bilayers may grow in to some more or less macroscopically large structure.

By considering Eq. (40) we may analyze the size of vesicles in terms of the three bending elasticity constants. The vesicle size is expected to slightly increase with decreasing values of k_cH_0. This may be explained as a result of the fact that the different contributions to k_cH_0 from the two oppositely curved monolayers, respectively, partly cancel one another. However, the outer layer is always more voluminous than the inner layer and, as a result, the net effect must be the vesicle size showing the same trend as a function of k_cH_0 as the outer layer. The bending rigidity has a large influence on vesicle size, in contrast to the case of spherical micelles and microemeulsion droplets. The reason for this has to do with the geometrical heterogeneous nature of vesicles. Increasing values of k_c favours a more uniformly curved geometry as the curvature of the outer and inner layers both approaches zero with increasing vesicle size. On the other hand, at low k_c -values the free energy penalty of accomplishing a large difference in curvature between the two layers is significantly reduced, allowing for comparatively small vesicles. As a matter of fact, rather small and thermodynamically stable vesicles have mainly been observed to be formed in surfactant mixtures, particularly in mixtures of two oppositely charged surfactants. (Tondre & Caillet, 2001) As previously mentioned, k_c is expected to be significantly reduced as two or more surfactants are mixed, and the magnitude of decrease is particularly pronounced in mixtures of oppositely charged surfactants. (Bergström, 2006b) Analogous to micelles, the aggregate size is expected to increase with increasing values of the saddle-splay constant, in accordance with the Gauss-Bonnet theorem.

10.2 Lamellar structures

The bending elasticity constants as the entire bilayer is regarded as an interface may be expressed in terms of the corresponding constants for a single monolayer, i.e. $H_0^{bi} = 0$, $k_c^{bi} = 2k_c$ and $\bar{k}_c^{bi} = 2\bar{k}_c - 8\xi k_c H_0$. (Porte et al., 1989; Szleifer et al., 1990; Ljunggren & Eriksson, 1992) Since H_0^{bi} is always zero for a thermodynamically equilibrated bilayer, more or less

macroscopic bilayer structures, with a mean curvature of the bilayer close to zero, are expected to be present as k_{bi} assumes large values.

The most common type of lamellar structure is ordered sheets of planar lamellar bilayers (L_α-phase). Since the two principal curvatures of planar geometry both equal zero ($c_1 = c_2 = 0$), it follows that $H = K = 0$ for the L_α-phase. However, another set of morphologies of bilayers with $H = ½(c_1 + c_2) = 0$ may be obtained by setting $c_1 = -c_2$. These kinds of bilayer interfaces, distinguished as having $H = 0$ and $K = c_1 \cdot c_2 < 0$, are examples of minimal surfaces. (Hyde et al., 1997) Macroscopic minimal surface bilayers are characterized as having a topology with $g \to \infty$. As a result, minimal bilayer interfaces ($g \to \infty$, $K < 0$) are favoured at the expense of macroscopic planar layers ($g = 0$, $K = 0$) by large values of $\bar{k}_c^{bi} = 2\bar{k}_c - 8\xi k_c H_0$. (Porte et al., 1989) Notably, low (possibly negative) values of the monolayer spontaneous curvature H_0 may cause $\bar{k}_c^{bi} > 0$, although $\bar{k}_c < 0$. Minimal bilayer interfaces may be both ordered (bicontinuous cubic lamellar structure, gyroids etc) and disordered (L_3-phase or "plumbers nightmare"). (Hyde et al., 1997) It may be noted that analogous monolayer structures (L_α-phase, L_3-phase, bicontinuous cubic structure etc) may be formed in oil/water/surfactant microemulsion systems as the monolayer spontaneous curvature $H_0 \approx 0$. (Jönsson et al., 1998).

The dependence of bilayer structure on the different bending elasticity constants are summarized in Table 2.

Bilayer systems ($H_0 < 1/4\xi$)	Small $\bar{k}_c$	Large $\bar{k}_c$
Small k_c	Small Vesicles	Disordered bilayers
Large k_c	Large Vesicles	Ordered bilayers

Table 2. The structural behaviour of self-assembled bilayers as a function of bending rigidity and saddle-splay constant

11. References

Ben-Shaul, A.; Szleifer, I. & Gelbart, W. M. (1985). Amphiphile Chain Organization in Micelles of Different Geometries. In: *Physics of Amphiphiles: Micelles, Vesicles and Microemulsions*, V. Degiorgio and M. Corti (Ed.), 404-428, North-Holland, ISBN: 978-0-44-486940-1, Amsterdam

Bergström, L. M. (2006a). *Langmuir*, 22, 3678-3691, ISSN: 0743-7463

Bergström, L. M. (2006b). *Langmuir*, 22, 6796-6813, ISSN: 0743-7463

Bergström, L. M. (2006c). *J. Colloid Interface Sci.*, 293, 181-193, ISSN: 0021-9797

Bergström, L. M. (2007). *ChemPhysChem*, 8, 462-472, ISSN: 1439-4235

Bergström, L. M. (2008a). *Colloids Surf. A*, 316, 15-26, ISSN: 0927-7757

Bergström, L. M. (2008b). *J. Colloid Interface Sci.*, 327, 191-197, ISSN: 0021-9797

Bergström, L. M. (2009). *Langmuir*, 25, 1949-1960, ISSN: 0743-7463

Bergström, L. M. & Bramer, T. (2008). *J. Colloid Interface Sci.*, 322, 589-595, ISSN: 0021-9797

Bergström, M. (2001a). *Langmuir*, 17, 993 - 998, ISSN: 0743-7463

Bergström, M. (2001b). Thermodynamics of Micelles and Vesicles. In: *Handbook of Surfaces and Interfaces of Materials*, H. S. Nalwa (Ed.), 233-264, Academic Press, ISBN: 0-12-513915-2, San Diego

Bergström, M. (2001c). *J. Colloid Interface Sci.*, 240, 294-306, ISSN: 0021-9797

Bergström, M. & Eriksson, J. C. (1996). *Langmuir*, 12, 624-634, ISSN: 0743-7463
Bergström, M. & Eriksson, J. C. (2000). *Langmuir*, 16, 7173-7181, ISSN: 0743-7463
Bergström, M.; Jonsson, P.; Persson, M. & Eriksson, J. C. (2003). *Langmuir*, 19, 10719-10725, ISSN: 0743-7463
Bergström, M. & Pedersen, J. S. (1999a). *Langmuir*, 15, 2250-2253, ISSN: 0743-7463
Bergström, M. & Pedersen, J. S. (1999b). *Phys. Chem. Chem. Phys*, 1, 4437-4446, ISSN: 1463-9076
Clint, J. H. (1975). *J. Chem. Soc., Faraday Trans. 1*, 71, 1327-1333, ISSN: 0300 -9599
Eriksson, J. C.; Ljunggren, S. & Henriksson, U. (1985). *J. Chem. Soc., Faraday Trans. 2*, 81, 833-868, ISSN: 0300-9238
Evans, D. F. & Wennerström, H. (1994). *The Colloidal Domain, Chapter 3*, Wiley-VCH, ISBN: 978-0-47-124247-5, New York
Flory, P. J. (1974). *Faraday Disc.*, 57, 7-29, ISSN: 0301-7249
Gruen, D. W. R. (1985). *J. Phys. Chem.*, 89, 153-163, ISSN: 1520-6106
Guggenheim, E. A. (1952). *Mixtures*, Clarendon Press, Oxford
Helfrich, W. (1973). *Z. Naturforsch. C*, 28, 693-703, ISSN: 0341-0382
Hill, T. L. (1963-64). *Thermodynamics of Small Systems (Parts I and II)*, Dover, ISBN: 0-486-68109-2, New York
Holland, P. M. (1992). Modeling Mixed Surfactant Systems. In: *Mixed Surfactant Systems*, P. M. Holland and D. N. Rubingh (Ed.), 31-51, American Chemical Society, ISBN: 978-0-84-122468-1, Washington, DC
Hyde, S.; Andersson, S.; Larsson, K.; Blum, Z.; Landh, T.; Lidin, S. & Ninham, B. W. (1997). *The Language of Shape*, Elsevier, ISBN: 978-0-444-81538-5, Amsterdam
Israelachvili, J. N. (1991). *Intermolecular and Surface Forces*, Academic press, ISBN: 978-0-12-375182, London
Israelachvili, J. N.; Mitchell, D. J. & Ninham, B. W. (1976). *J. Chem. Soc., Faraday Trans. 2*, 72, 1525-1568, ISSN: 0300-9238
Jönsson, B.; Lindman, B.; Holmberg, K. & Kronberg, B. (1998). *Surfactant and Polymers in Aqueous Solution*, Wiley, ISBN: 978-0-47-149883-4, Chichester
Kozlov, M. M. & Helfrich, W. (1992). *Langmuir*, 8, 2792-2797, ISSN: 0743-7463
Ljunggren, S. & Eriksson, J. C. (1992). *Langmuir*, 8, 1300, ISSN: 0743-7463
Mitchell, D. J. & Ninham, B. W. (1989). *Langmuir*, 5, 1121-1123, ISSN: 0743-7463
Porte, G. (1992). *J. Phys.: Condens. Matter*, 4, 8649-8670, ISSN: 0953-8984
Porte, G.; Appell, J.; Bassereau, P. & Marignan, J. (1989). *J. Phys. France*, 50, 1335-1347, ISSN: 1155-4304
Porte, G. & Ligoure, C. (1995). *J. Chem. Phys.*, 102, 4290-4298, ISSN: 0021-9606
Safran, S. A. (1991). *Phys. Rev. A*, 43, 6, 2903-2904, ISSN: 0556-2791
Safran, S. A. (1999). *Adv. Phys.*, 48, 4, 395-448, ISSN: 0001-8732
Shinoda, K.; Nakagawa, T.; B.-I., T. & Isemura, T. (1963). *Colloidal Surfaces*, Academic Press, New York and London
Szleifer, I.; Kramer, D.; Ben-Shaul, A.; Gelbart, W. M. & Safran, S. A. (1990). *J. Chem. Phys.*, 92, 6800-6817, ISSN: 0021-9606
Tanford, C. (1980). *The hydrophobic effect*, Wiley, ISBN: 978-0-47-104893-0, New York
Tondre, C. & Caillet, C. (2001). *Adv. Colloid Interface Sci.*, 93, 115-134, ISSN: 0001-8686

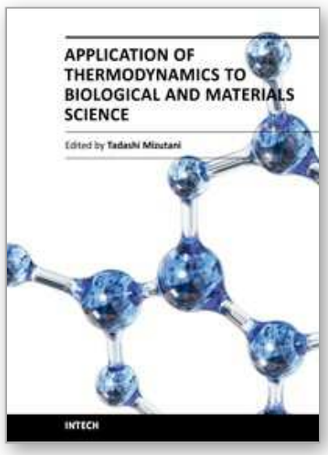

Application of Thermodynamics to Biological and Materials Science

Edited by Prof. Mizutani Tadashi

ISBN 978-953-307-980-6
Hard cover, 628 pages
Publisher InTech
Published online 14, January, 2011
Published in print edition January, 2011

Progress of thermodynamics has been stimulated by the findings of a variety of fields of science and technology. The principles of thermodynamics are so general that the application is widespread to such fields as solid state physics, chemistry, biology, astronomical science, materials science, and chemical engineering. The contents of this book should be of help to many scientists and engineers.

How to reference

In order to correctly reference this scholarly work, feel free to copy and paste the following:

L. Magnus Bergström (2011). Thermodynamics of Self-Assembly, Application of Thermodynamics to Biological and Materials Science, Prof. Mizutani Tadashi (Ed.), ISBN: 978-953-307-980-6, InTech, Available from: http://www.intechopen.com/books/application-of-thermodynamics-to-biological-and-materials-science/thermodynamics-of-self-assembly

INTECH
open science | open minds

InTech Europe
University Campus STeP Ri
Slavka Krautzeka 83/A
51000 Rijeka, Croatia
Phone: +385 (51) 770 447
Fax: +385 (51) 686 166
www.intechopen.com

InTech China
Unit 405, Office Block, Hotel Equatorial Shanghai
No.65, Yan An Road (West), Shanghai, 200040, China
中国上海市延安西路65号上海国际贵都大饭店办公楼405单元
Phone: +86-21-62489820
Fax: +86-21-62489821

IntechOpen